Title
Fine-tuning robot-assisted radical prostatectomy planning with MRI

Journal
Urologic Oncology Seminars and Original Investigations, 31(6)

ISSN
1078-1439

Authors
Finley, David S
Margolis, Daniel
Raman, Steve S
et al.

Publication Date
2013-08-01

DOI
10.1016/j.urolonc.2011.07.013

Peer reviewed

ELSEVIER

Urologic Oncology: Seminars and Original Investigations 31 (2013) 766–775

UROLOGIC ONCOLOGY

Original article

Fine-tuning robot-assisted radical prostatectomy planning with MRI

David S. Finley, M.D.[a,*], Daniel Margolis, M.D.[b], Steve S. Raman, M.D.[b], Benjamin M. Ellingson, Ph.D., M.S.[b], Shyam Natarajan, Ph.D.[c], Nelly Tan, M.D.[b], Jiaoti Huang, M.D., Ph.D.[d], Robert E. Reiter, M.D., MBA[e]

[a] *Department of Urology, Kaiser Permanente Los Angeles Medical Center, Los Angeles, CA 90027, USA*
[b] *Department of Radiology, David Geffen School of Medicine at UCLA, Los Angeles, CA 90095, USA*
[c] *Department of Biomedical engineering, David Geffen School of Medicine at UCLA, Los Angeles, CA 90095, USA*
[d] *Department of Pathology, David Geffen School of Medicine at UCLA, Los Angeles, CA 90095, USA*
[e] *Department of Urology, David Geffen School of Medicine at UCLA, Los Angeles, CA 90095, USA*

Received 9 May 2011; received in revised form 22 July 2011; accepted 25 July 2011

Abstract

Objectives: Robot-assisted radical prostatectomy (RARP) has now become the most common surgical treatment option for prostate cancer (CaP). Clinicopathologic data (i.e., biopsy, digital rectal exam, prostate specific antigen level) and patient-specific factors (e.g., age, erectile function, co-morbidities) are the primary sources of information that urologists use for counseling and treatment decision making. Magnetic resonance imaging (MRI) has evolved along a similar temporal arc to RARP, with increased utilization and precision over the past decade. MRI prior to RARP provides multifaceted adjunctive information, including enhancement of locoregional staging, delineation of spatial anatomic information, and identification of aberrant anatomy, all of which aid in patient treatment counseling and operative planning. This article is designed for urologic surgeons who perform RARP, with the aim of providing a review of prostate MRI imaging and highlighting findings which may specifically alter the operation.

Methods and materials: A review of the literature was performed, focusing on the most recent publications.

Results: MRI imaging of the prostate has become increasing accurate for the identification, localization, and characterization of CaP lesions. In addition to tumor-specific information, a number of intra- and extra-prostatic findings are consistently identified on MRI which may impact RARP.

Conclusions: MRI provides important information which may alter RARP.

Keywords: Robotic-assisted radical prostatectomy; RALP; RARP; Magnetic resonance imaging; MRI; Multiparametric

1. Introduction

Robot-assisted radical prostatectomy (RARP) has now become the most common surgical treatment option for prostate cancer (CaP). Most surgeons rely on the combination of prostate needle biopsy, serum prostate specific antigen (PSA), and digital rectal exam (DRE) findings in combination with patient-specific baseline characteristics (e.g., age, erectile function, BMI, co-morbidities) for patient counseling and treatment decision-making. Although this information lateralizes the tumor and can be entered into standard nomograms to predict pathologic findings, it relies on imperfect and varied biopsy sampling techniques, which suffer from inadequate spatial anatomic information. Given the absence of haptic feedback among current robotic platforms and the surgeon's reliance upon intra-operative visual cues during RARP, the supplemental information provided by preoperative multiparametric endorectal coil MRI (mp-eMRI) imaging may help fill this void by acting as a surrogate for tactile information. Neither computed-tomography (CT) nor ultrasound is adequate in this setting, providing insufficient contrast between benign and malignant tissue [1]. mp-eMRI of the prostate provides enhanced locoregional staging, which not only aids in the selection of treatment options for patients but also provides essential anatomic information allowing for precise operative planning. For example, patients with minimal disease on biopsy whose subsequent MRI is concordant may opt for enrollment in a surveillance protocol whereas patients with evidence of extraprostatic extension (EPE) (Fig. 1) may undergo wide

* Corresponding author. Tel.: (323) 783-5865; fax: (323) 783-7272.
E-mail address: finds7@gmail.com (D.S. Finley).

1078-1439/$ – see front matter
doi:10.1016/j.urolonc.2011.07.013

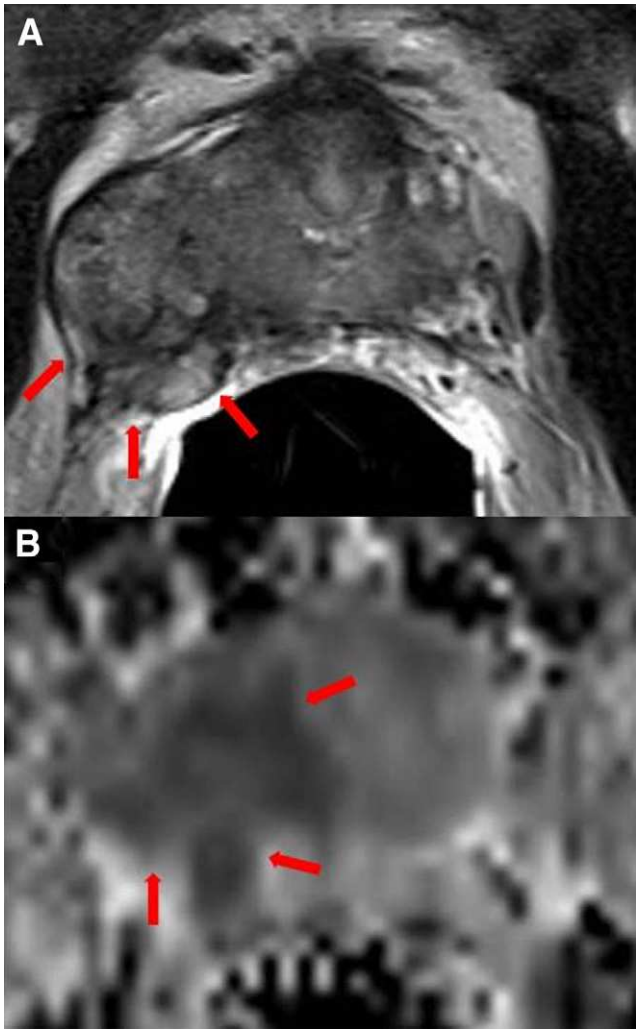

Fig. 1. Gross extraprostatic extension on the right seen on T2WI (A) and DWI (B). (Color version of figure is available online.)

excision. For patients who are deemed to be acceptable surgical candidates by MRI and clinicopathologic information, a number of key findings are consistently demonstrated on imaging, which may enable the surgeon to optimize pathologic and functional outcomes by modifying particular surgical steps during RARP. In addition, incidental extraprostatic findings such as inguinal hernia are occasionally found, which may impact the surgical plan or prevent reoperation. In this article, we will provide a brief review of mp-eMRI imaging and discuss the findings that may affect intra-operative decision and facilitate the operation.

2. Multiparametric MRI

Prostate MRI has yet to be widely adopted by most centers primarily because its rapid evolution and non-standardized technique has generated mixed reports on its accuracy and utility in clinical practice [2]. Over the past decade, prostate MRI has dramatically improved, providing the surgeon with an increasing degree of anatomic spatial resolution and functional information, which enables precise tumor mapping [3]. The latest MRI platforms and sequences have generated an unprecedented level of anatomic detail and tumor specificity. Despite this, there are valid concerns with cost-effectiveness and reimbursement. In an effort to address these issues and establish baseline uniformity, experts in the fields of CaP and prostate MRI recently convened to generate consensus recommendations regarding MRI protocol and reporting [2]. Furthermore, recent German recommendations include MRI of the pelvis prior to treatment decision making in men with high risk disease [4].

At our center, we routinely obtain anatomic T1 (T1WI) and multiplanar T2-weighted imaging (T2WI), diffusion weighted imaging (DWI) with apparent diffusion coefficient (ADC) map, dynamic contrast enhancement (DCE), diffusion-tensor imaging (DTI), and MR spectroscopic imaging (MRSI), combined into a composite study termed mp-eMRI. An endorectal coil, although not essential, is preferred because it acts as an antenna to increase the signal-to-noise ratio. As a result, enhanced image resolution is obtained on T2WI, as well as improved fidelity of DWI and higher spectral integrity for MRSI [3,5]. In addition, at the present time, the study is optimally generated with a 3.0 Tesla magnet with slice thickness $\leq$ 3.0 mm. If an endorectal coil is not available, external phased-array imaging at 3.0 Tesla (T) is recommended, which provides slightly inferior image quality compared with 1.5T eMRI but does not affect diagnostic accuracy [6].

The exam is scheduled approximately 6 to 8 weeks after biopsy to minimize hemorrhage artifact. Hong et al. found that RARP performed within 2 weeks of biopsy was more difficult in cases with increased biopsy-associated hemorrhage as measured by T1WI [7]. We also instruct the patient to abstain from intercourse for 48 hours prior to the study to distend the seminal vesicles enhancing radiographic inspection. The morning of the exam, a self-administered fleet's enema is taken and the patient takes a short-acting benzodiazepine an hour before the study to minimize claustrophobia. Glucagon is administered intramuscularly as an anti-peristaltic to reduce motion artifact, regardless of whether an endorectal coil is used.

To be sure, the learning curve for prostate MRI is steep, similar to breast MRI or virtual colonography, requiring a fellowship trained radiologist. While the multiparametric approach and appearance of suspicious and benign findings are dissimilar from most other cross sectional imaging, the increasing popularity of online and conference-based workshops on prostate MRI suggests that there is growing interest in the radiological community in honing this skill.

2.1. Anatomic sequences: T1 and T2 weighted imaging

The most elementary sequences are conventional T1 and T2WI, which provide images with the best spatial resolution and zonal anatomic detail. T1 images are primarily used to evaluate for bright (hyperintense) areas of hemorrhage, but can also evaluate lymph node and bone marrow status. T2WI is the optimal sequence to initially identify and spatially triangulate tumor location within the prostate gland, which typically appear as a dark (hypointense) round, ovoid, or irregular shaped area without corresponding hemorrhage on T1. False positive areas may occur due to prostatitis, scar tissue, calcium, and other factors [8]. Central gland imaging tends to be more difficult due to the heterogeneous appearance of benign prostatic hyperplasia (BPH); this issue may have minimal relevance to patients undergoing RARP, however.

The precise location of the lesion is mapped in axial, sagittal, and coronal planes, peripheral or central gland location, anterior/posterior, distance from prostate capsule, capsular contact or bulge or extraprostatic extension, and proximity to neurovascular bundle (NVB). In this regard, MRI imaging is essentially an advanced three-dimensional digital rectal exam. Once a potential lesion is identified on T2WI, functional imaging sequences are cross-referenced for corroborating data (see below). Importantly, T2WI as a stand-alone sequence does have limitations with regard to image resolution of small tumors. Roethke et al. reported that T2W eMRI was able to detect 0%. 3%, 13%, 45%, and 89% of lesions measuring □ 0.3 cm, 0.3–0.5 cm, 0.5–1.0 cm, 1.0–2.0 cm, and □ 2.0 cm, respectively [9]. Others have noted variation in the sensitivity and specificity according to prostate topography [8]. Colleselli et al. compared T2W eMRI against whole mount prostatectomy specimens and found that the highest sensitivity for tumor detection occurred in the dorsal base of the prostate and the lowest in the ventral apex [8]. Due to these potential limitations, T2WI is not used in isolation, but rather in the context of the other sequences in the mp-eMRI study, which enhance the overall sensitivity and specificity for tumor staging [10]. In addition, detection of small tumors may be more relevant for patients on active surveillance or for planning of focal therapy than for surgical planning.

2.2. Functional sequences: DWI, DCE, MRSI

DWI is acquired by application of a pulsed magnetic field gradient, which is sensitive to free water proton movement (i.e., Brownian motion of water molecules), creating image contrast that can be measured and quantified [2,11]. Water diffusion is generally restricted in cancerous tissue due to dense cellular packing and abnormal cell membrane architecture [2,12]. Hypercellular regions with restricted diffusion appear darker (hypointense) on the ADC map, which inversely correlates with the probability (and likely grade) of cancer. It is important to note that the free diffusion of water can also be restricted from non-cancerous factors such as fibrosis and glandular organization [13,14]. In general, values □ 1.4 □ 10^{-3} mm^2/s are considered to be suspicious for cancer [10,11]. Recent data has indicated that ADC values exhibit an inverse relationship to Gleason grade [11]. The group from Nijmegen, based on receiver operating characteristic (ROC) analysis, found high discriminatory performance for differentiating low grade from higher grade lesions; the median ADC for low grade, intermediate grade, and high-grade tumors was 1.30, 1.07, and 0.94 □ 10^{-3} mm^2/s, respectively. Others have shown that for lesions located in the central gland, the inverse relationship between ADC and Gleason grade does not hold up due to cellular heterogeneity of BPH tissue [15]. Thus, a hypointensity in the peripheral zone identified on T2WI with a low ADC value on DWI indicates a likely area of cancer and provides information on the aggressiveness of the lesion. This information is adjunctive to tumor grade identified on biopsy which is upgraded in approximately 40% of RP specimens [16,17].

DCE sequences are obtained following gadolinium-based contrast administration (e.g., gadopentetate dimeglumine) using a power injector for intravenous administration to obtain tissue perfusion information. Contrast agent diffusion through cancerous tissue is often increased due altered tumor cellular architecture, neovascularity, and increased vascular permeability [18]. Qualitative enhancement is assessed and contrast agent uptake (wash-in) and clearance (wash-out) can be quantified by the pharmacokinetic parameters K^{trans} (volume transfer constant) and K_{ep} (rate constant), respectively. Prostate tumors characteristically display intense early enhancement with rapid washout compared with benign prostate tissue due to a relatively larger extracellular space [18–20]. The combination of DWI, DCE, and T2WI appears to have the highest sensitivity and specificity for staging of tumors [10,21–24]. Fig. 2 depicts representative images of these functional sequences.

MR spectroscopy (MRSI) provides additional functional information by exploiting the metabolic differences between benign and cancerous tissue [25]. Malignant prostate tissue characteristically displays a biochemical signature with elevated choline (due to high cell membrane turnover) and decreased citrate levels compared to benign tissue [26,27]. The choline-plus-creatine-to-citrate ratio (CC/C-ratio) [28] or simply the choline:citrate ratio [29] is the main metabolic criterion that is used to identify cancer. A choline/creatine peak height $\geq$ 2 times the citrate peak height is highly suspicious for cancer [30]. Importantly, this relationship has been demonstrated for both peripheral zone lesions and central gland lesions, unlike DWI [31,32]. Riches et al. found a mean choline:citrate ratio of 0.35 in cancerous prostate tumors $\geq$ 1 cm compared with 0.11 in benign tissue [32]. Zakian et al. found a direct correlation between CC/C-ratio and Gleason score for peripheral zone lesions (e.g., elevated choline level and reduction of citrate level as a function of increasing cancer aggressiveness) [33]. Thus,

MRSI, like DWI ADC mapping, can provide information regarding the aggressiveness of the tumor which factors in with the other information used in CaP treatment planning.

3. RARP geared MRI Reporting

Our genitourinary radiologists structure prostate MRI reports for intra-operative ease of use to maximize tumor localization and surgical decision making in three dimensions (Fig. 2). In addition to standard reporting components (e.g., tumor size, presence of seminal vesicle invasion etc.), spatial anatomic information is provided for the surgeon to reference during RARP [axial clock-face tumor location (e.g., 7ϖ'clock), capsular distance, distance from apex to base (e.g., 30%)]. The degree of neoplasia confidence and aggressiveness is provided based on the global assessment of the T2 weighted images, MRSI, and quantitative parameters ADC, K_{ep}, K^{trans}.

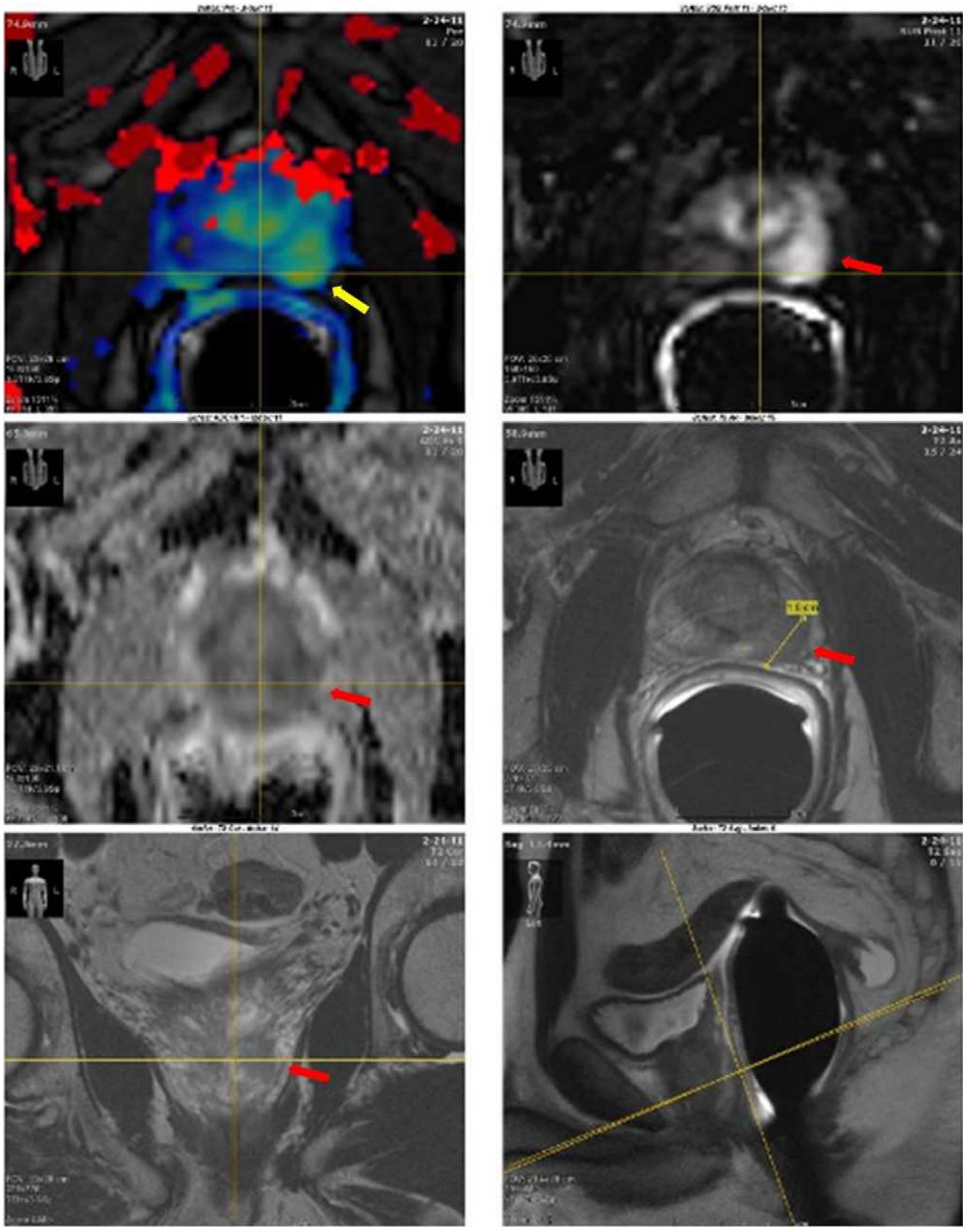

Fig. 2. Composite (or collage) images for localization. (A) Color perfusion map and (B) wash-in perfusion map are highly abnormal (arrows) whereas (C) the apparent diffusion coefficient map of diffusion weighted imaging shows only slightly restricted diffusion (darker signal). Each of these 3 components serves to rank the suspicion for cancer, and the degree to which they are abnormal suggests the grade of disease. The T2-weighted images in (D) transaxial, (E) coronal, and (F) sagittal orientation, which have higher spatial resolution but are less specific, identify both the level and location of the tumor, its size, and potential involvement of the capsule. A mid-sagittal image rather than a co-localized sagittal image is chosen to better identify the level, from apex to base, where the tumor lies. (Color version of figure is available online.)

4. Modifiable surgical steps based on specific MRI findings

4.1. Neurovascular bundle sparing

The decision to preserve or resect the NVB at surgery has historically relied on factors including baseline erectile function of the patient, digital rectal exam and/or ultrasound findings, biopsy results, and intra-operative assessment of the NVB based on direct palpation, frozen section, and/or visual cues. The accuracy of direct proprioceptive evaluation or an "abnormal" nontactile appearance of the NVBs during their release is controversial. In addition, the factors that affect positive surgical margin rates are complex and unreliably defined under nonrandomized controlled conditions. Despite this, some limited information exists. For example, Rapp et al. decided to preserve or widely excise the NVB at open RRP based in part on intra-operative examination of the bundle [34]. In this retrospective series, 49/403 of men (12%) had an apparent palpable abnormality in the region of the NVB and therefore underwent ipsilateral wide excision. On final pathology, EPE was detected in 37% of resected bundles resulting in a single positive surgical margin. Among the remaining 354 patients who underwent bilateral nerve sparing based on a "normal" intra-operative prostate assessment, 8.5% were found to have EPE of the NVB with a corresponding PSM rate of 23%. Thus, although palpation may have picked up some cases of extraprostatic disease in this series contributing to a low positive surgical margin rate, clearly its sensitivity for detecting EPE is low resulting in unnecessary NVB resection in the majority of cases.

For the radical prostatectomist, by far the most important information mp-MRI potentially provides is tumor localization and mapping relative to the NVB(s) allowing for alteration of nerve sparing dissection in an incremental nerve sparing approach. Whereas complete interfascial (i.e., between the prostatic fascia and levator fascia) nerve sparing is usually performed for tumors that are lower grade and distant from the prostatic capsule, those with broad-based capsular contact, capsular bulging, or irregularity in the region of NVB are generally amenable to partial NVB resection (Fig. 3). In the

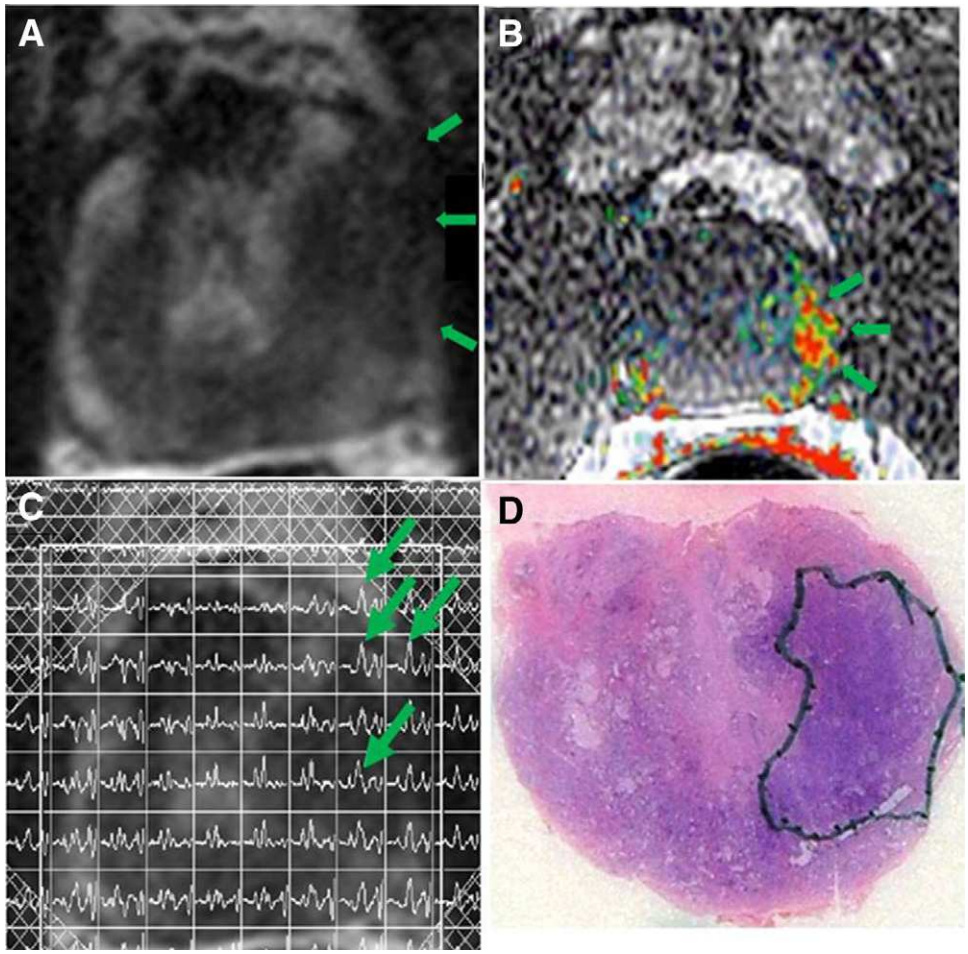

Fig. 3. (A) Transaxial T2-weighted image showing anterolateral tumor (arrows) that spares the rectoprostatic angle. (B) Color perfusion map and (C) spectroscopic overlay image are mildly abnormal at the level of the tumor, confirming that this reflects neoplasia and not sequelae of prostatitis. (D) Whole-mount prostatectomy specimen at the same level revealing tumor sparing the rectoprostatic angle. (Color version of figure is available online.)

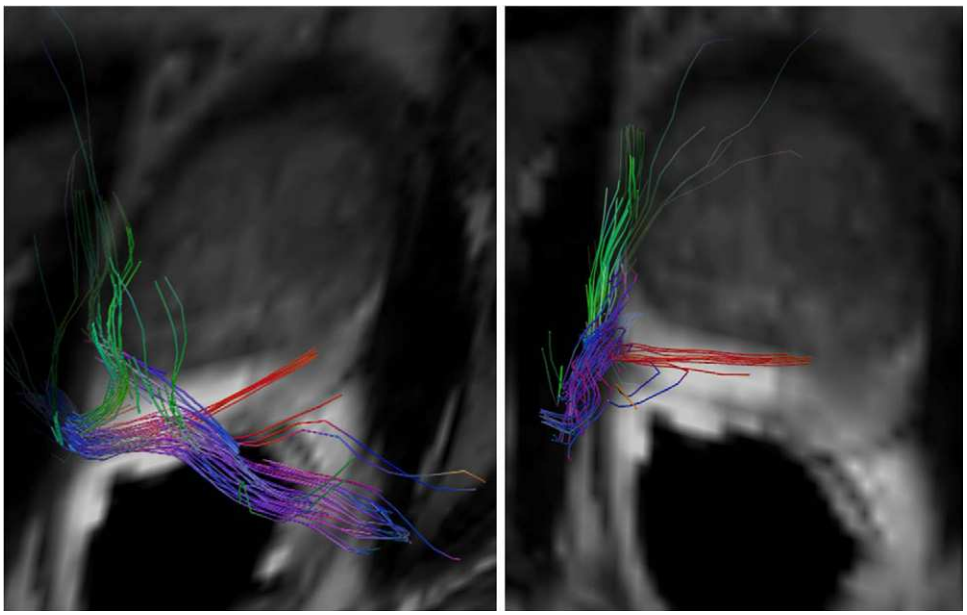

Fig. 4. Three-dimensional diffusion-tensor imaging overlaid on oblique and semi-oblique images of the prostate. Fiber tracks are color-coded based on direction, yellow-green being anteroposterior, red-orange being transverse, and blue-purple for craniocaudal. These images show the majority of fiber tracks in craniocaudal orientation along the rectoprostatic angle, with a few fibers extending anteriorly and some crossing fibers contralaterally. (Color version of figure is available online.)

setting of suspected EPE based on mp-eMRI, a partial or complete extra-fascial excision (en bloc resection of all tissue anterior to the rectal surface) may be performed. Conversely, in cases where MRI predicts an absence of tumor in the region of the NVB, the surgeon and patient are reassured of the decision for nerve sparing. Several studies have attempted to quantify the accuracy and value of MRI in this decision making process [35–38]. Hricak et al. generated a presurgical plan for dealing with the NVB at open RP based on standard (i.e., biopsy information, DRE, PSA) and then with the addition of 1.5T T2WI-eMRI information for 135 patients [36]; a 5-point scale based on the degree of planned NVB preservation (1 □ definite preservation, 5 □ definite resection) was used to assign a numeric score to the pre-MRI and post-MRI plans. Bilateral nerve sparing, partial nerve sparing, and complete nerve resection was performed in 223 NVBs, 7 NVBs, and 40 NVBs, respectively. Overall, MRI resulted in an alteration of the surgical plan for 39% of NVBs. Among a subset of patients with a high probability of EPE (according to the Partin staging tables), MRI was found to change the NVB management in 78% of cases, 93% of which were deemed to be appropriate based on histopathologic assessment. Within this subset of men, MRI correctly suggested NVB preservation in 83%, "saving" the patient from unnecessary resection. Overall, a statistically significant increase in the area under the curve (generated from ROC curves) for the accuracy of surgical judgment based on MRI information was found compared to clinical factors alone (0.832 vs. 0.741, respectively). In a related study, Margolis et al. evaluated the utility of1.5T mp-eMRI among 104 men undergoing RARP [39]. In this predominantly pT2 patient population, the authors found an MRI-driven change in nerve-sparing in 28% of cases. No positive surgical margins occurred in patients whose surgical plan was changed to a non-nerve-sparing procedure whereas only 1 positive margin occurred in a patient changed to a nerve-sparing technique. The specificity for MRI to differentiate between pT2 and pT3 disease was 97.5%. Despite these intriguing data, large prospective studies with a wide stage distribution are warranted to better determine whether or not surgical margin rates can be directly reduced with the addition of MRI information.

Emerging MRI techniques such as diffusion-tensor imaging (DTI), an MRI sequence that quantifies the magnitude and direction of water self-diffusion, can elegantly visualize the rich neurovascular network around the prostate (Fig. 4), highlighting the location of the NVBs relative to the tumor, which may further enhance surgical planning [2]. Thus, mp-eMRI provides the surgeon with adjunctive information beyond standard clinical criteria, which aids in creating a "game-plan" for NVB sparing. In low-risk cases, this information reassures the surgeon and patient that nerve-sparing is likely to be appropriate; for higher-risk patients, MRI may confirm the need for a wide(r) resection to maximize oncologic control.

4.2. Anterior apical and posterior dissection

Incomplete cancer removal resulting in a positive surgical margin at RP is recognized by most as an independent risk factor for biochemical recurrence [40–42]. The most common locations for positive surgical margins are at the apex and posterolaterally, adjacent to the NVB [40,43,44].

Extraprostatic extension often coincides with the site of a positive surgical margin [40]. In this regard, additional tissue may be preemptively resected in this high-risk area. In cases in which a low grade tumor is located distant from the capsule, the posterior dissection can be safely completed between the leaflets of Denonvillier's fascia; this posterior layer is included in the posterior reconstruction which may promote continence recovery [45,46]. However, Denonvillier's fascia invasion occurs in up to 13% of cases [47]. When MRI indicates a lesion is situated in the peripheral zone in contact with the posterior capsule, we carefully redirect our dissection plane outside the leaflets of Denonvillier's fascia in the pre-rectal cleavage plane rather than between the layers to gain an extra margin of tissue.

Tumors of the anterior prostate occur in approximately 15% of cases, a region that is difficult to adequately sample by needle biopsy [48]. MRI may identify tumors in this location more reliably than transrectal ultrasound [49,50]. For tumors that are located at the anterior apex, at the time of RARP, we perform a more extensive apical dissection, which includes wide resection of the anterior prostatic fat pad [51,52]. In addition, a slightly more distal urethral margin may be advisable for some apical tumors [53]. A more aggressive apical dissection may translate to a reduction in positive surgical margin rates in this location [54]. Whether or not surgical modification to deal with apical tumors identified by mp-MRI directly reduces margin rates awaits further study.

4.3. Median lobe and aberrant anatomy

Sagittal plane T2WI provides an excellent view of the prostate to determine whether a significant median lobe is present (Fig. 5). Although the presence of prostatic tissue protruding into the bladder neck may be detected on ultrasound or readily apparent during the bladder neck dissection step, in some cases the presence and size of the median lobe can be difficult to assess. A priori knowledge of a large median lobe is valuable and can expedite the bladder neck resection and/or reconstruction step.

mp-eMRI also can identify the presence of anomalous accessory apical and lateral pudendal arteries, which occur in approximately one-third of patients (range 4%–75%), Fig. 6A [55,56]. Although some data indicate that sacrifice of APAs in patients with normal preoperative erectile function has no discernible impact on recovery of potency [57], some authors recommend artery sparing whenever possible [58]. Indeed, in approximately 20% of patients, this arterial inflow may be the dominant blood supply to the penis [56]. In our experience, we attempt to spare APAs whenever possible for men with borderline baseline erectile function. Patients in whom MRI detects an APA are counseled accordingly regarding the potential risks.

4.4. Pelvic anatomy and prediction of surgical difficulty

Nguyen et al. used eMRI to measure pelvic and prostate dimensions to predict surgical difficulty during RARP [59]. The ratio of the prostate diameter to pelvic cavity index (PCI) correlated with surgical difficulty (EBL, transfusion rate, operative time, positive surgical margin rate) on multivariate analysis. Patients with large prostates situated within deep narrow pelvises were associated with the most operative difficulty. Mason et al. reported a similar association between surgical difficulty, prostate size, and pelvic width and depth [60]. Von Bodman and colleagues, however, found no correlation between pelvic dimensions or intrapelvic prostate location on preoperative MRI and surgical complications [61]. In

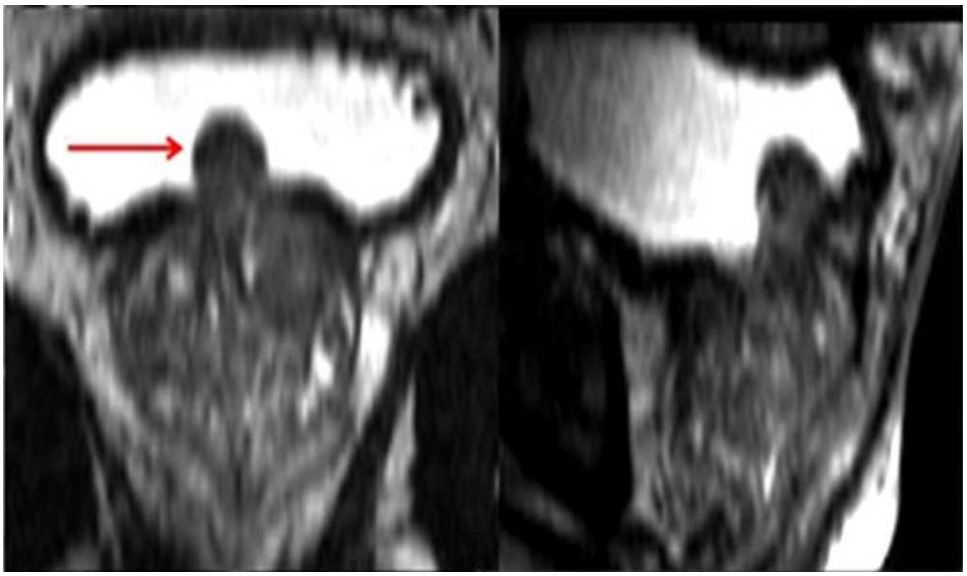

Fig. 5. Median lobe on coronal and sagittal imaging. (Color version of figure is available online.)

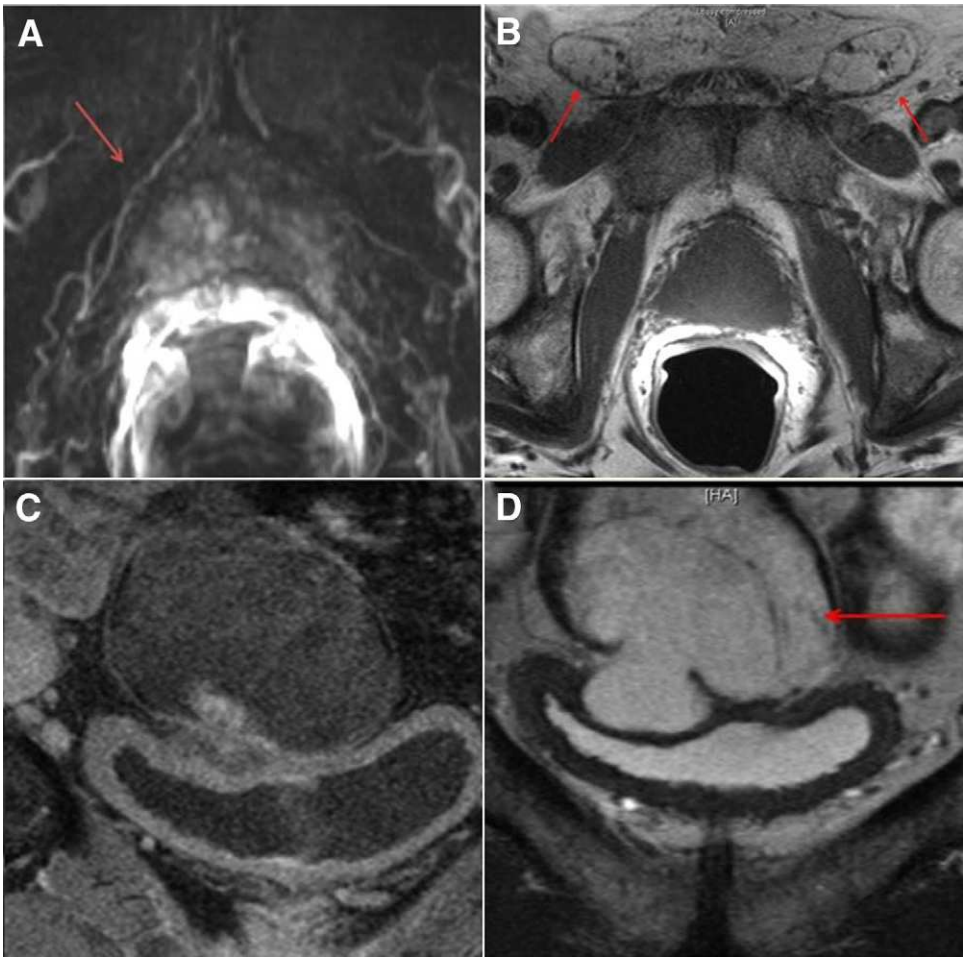

Fig. 6. Lateral accessory APA (A), bilateral inguinal hernias (B), incidental findings: urachal mass (C), (D). (Color version of figure is available online.)

another study by Mendoza and colleagues, preoperative eMRI was used to measure urethral length, urethral sphincter characteristics, and prostate size which were correlated to post RARP time to continence in a multivariate model [62]. A longer urethral length and larger prostate size on eMRI were found to be independent factors associated with time to recovery of continence. The authors concluded that preoperative eMRI was a valuable tool for patient counseling which effectively factors in to the treatment decision making process.

4.5. Incidental findings

In addition to evaluation of pelvic lymph nodes [63], mp-eMRI can occasionally detect incidental findings that may require attention during surgery. For example, inguinal hernia occurs in approximately 25% of patients undergoing RARP [64]. Although some overt hernias can be detected on preoperative clinical exam, others are subclinical and discovered at the time of surgery. Preoperative MRI imaging is a sensitive method for the detection of pre-existent occult inguinal hernia that allows for preoperative counseling and preparation for concurrent intra-operative repair (Fig. 6B), [65]. Given that many subclinical hernias progress to overt hernias, repair at the time of RARP saves reoperation in a significant percentage of cases.

In addition to inguinal hernias, other less common pathology is encountered on preoperative imaging that may demand modification of the surgical plan. For example, a large urachal mass was found, which was subsequently resected at the time of RARP; pathology demonstrated a well-differentiated urachal adenocarcinoma (Fig. 6C, D). Rarely, bladder pathology (e.g., tumors, diverticula, Wolffian duct derivative anomalies, ectopic or duplicated ureters, or adenocarcinoma of the seminal vesicle may also be found [66,67]. Although in some circumstances these findings may not require intervention or might be dealt with if encountered unexpectedly at the time of surgery, advanced knowledge based on imaging may aid in appropriate counseling and planning.

5. Conclusion

Although prostate MRI has evolved and matured along a similar timeline as RARP, it has yet to be routinely integrated

into surgical planning at most centers for a variety of reasons. While mp-eMRI is still imperfect for the mapping of small, low-grade tumors, larger and higher grade tumors are now routinely identified that correlate well with whole-mount pathology. Recent data have demonstrated that mp-eMRI provides value for staging, treatment decision-making, and operative planning. mp-eMRI can also identify abnormal anatomy and pathology that may facilitate or modify RARP. Armed with this supplemental information, urologic surgeons may ultimately perform more precise operations and improve patient outcomes. Before recommendations regarding its routine use can be made, mp-MRI is still being performed under investigational status pending further evaluation of the newer functional sequences, cost/benefit analysis, and determination of optimal patient selection.

References

[1] Fuchsjäger M, Shukla-Dave A, Akin O, et al. Prostate cancer imaging. Acta Radiol 2008;49:107–20.

[2] Dickinson L, Ahmed HU, Allen C, et al. Magnetic Resonance imaging for the detection, localization, and characterization of prostate cancer: Recommendations from a European Consensus Meeting. Eur Urol 2011;59:477–94.

[3] Sciarra A, Barentsz J, Bjartell A, et al. Advances in magnetic resonance imaging: How they are changing the management of prostate cancer. Eur Urol 2011;59:962–7.

[4] Grimm MO, Thomas C, Frohner M, et al. Pelvic lymphadenectomy and radical prostatectomy. Recommendations of the German S3 Guideline. Urologe A 2010;49:206–10.

[5] Yakar D, Heijmink SW, Hulsbergen-van de Kaa CA, et al. Initial results of three-dimensional 1H-magnetic resonance spectroscopic imaging in the localization of prostate cancer at 3 Tesla: Should we use an endorectal coil? Invest Radiol 2011;46:301–6.

[6] Torricelli P, Barberini A, Cinquantini F, et al. 3-T MRI with phased-array coil in local staging of prostatic cancer. Acad Radiol 2008;15: 1118–25.

[7] Hong SK, Kim DS, Lee WK, et al. Significance of post-biopsy hemorrhage observed on preoperative magnetic resonance imaging in performing robot-assisted laparoscopic radical prostatectomy. World J Urol 2010;28:721–6.

[8] Colleselli D, Schilling D, Lichy MP. Topographical sensitivity and specificity of endorectal coil magnetic resonance imaging for prostate cancer detection. Urol Int 2010;84:388–94.

[9] Roethke MC, Lichy MP, Jurgschat L, et al. Tumor size dependent detection rate of endorectal MRI of prostate cancer: Histopathologic correlation with whole-mount sections in 70 patients with prostate cancer. Eur J Radiol 2010, Mar 11 [Epub ahead of print].

[10] Delongchamps NB, Rouanne M, Flam T, et al. Multiparametric magnetic resonance imaging for the detection and localization of prostate cancer: Combination of T2-weighted, dynamic contrast-enhanced and diffusion-weighted imaging. BJU 2010;107:1411–8.

[11] Hambrock T, Somford DM, Huisman HJ, et al. Relationship between apparent diffusion coefficients at 3.0-T MR imaging and Gleason grade in peripheral zone prostate cancer. Radiology 2011; 259:453–61.

[12] Uhl M, Altehoefer C, Kontny U, et al. MRI-diffusion imaging of neuroblastomas: First results and correlation to histology. Eur Radiol 2002;12;2335–8.

[13] Chenevert TL, Sundgren PC, Ross BD. Diffusion imaging: Insight to cell status and cytoarchitecture. Neuroimaging Clin N Am 2006;16: 619–32.

[14] Langer DL, van der Kwast TH, Evans AJ, et al. Prostate tissue composition and MR measurements: Investigating the relationships between ADC, T2, K(trans), v(e), and corresponding histologic features. Radiology 2010;255:485–94.

[15] Verma S, Rajesh A, Morales H, et al. Assessment of aggressiveness of prostate cancer: Correlation of apparent diffusion coefficient with histologic grade after radical prostatectomy. AJR 2011;196:374–81.

[16] Bostwick DG. Gleason grading of prostate needle biopsies: Correlation with grade in 316 matched prostatectomies. Am J Surg Pathol 1994;18:796–803.

[17] Corcoran NM, Hong MK, Casey RG, et al. Upgrade in Gleason score between prostate biopsies and pathology following radical prostatectomy significantly impacts upon the risk of biochemical recurrence. BJU Int 2011, Mar 28 [Epub ahead of print].

[18] Noworolski SM, Henry RG, Vigneron DB, et al. Dynamic contrast-enhanced MRI in normal and abnormal prostate tissues as defined by biopsy, MRI, and 3D MRSI. Magn Reson Med 2005;53:249–55.

[19] McMahon CJ, Bloch BN, Lenkinski RE, et al. Dynamic contrast-enhanced MR imaging in the evaluation of patients with prostate cancer. Magn Reson Imaging Clin N Am 2009;17:363–83.

[20] Isebaert S, De Keyzer F, Haustermans K, et al. Evaluation of semi-quantitative dynamic contrast-enhanced MRI parameters for prostate cancer in correlation to whole-mount histopathology. Eur J Radiol 2011 Feb 22 [Epub ahead of print].

[21] Kitajima K, Kaji Y, Fukabori Y, et al. Prostate cancer detection with 3 T MRI: Comparison of diffusion-weighted imaging and dynamic contrast-enhanced MRI in combination with T2-weighted imaging. J Magn Reson Imaging 2010;31:625–31.

[22] Vargas HA, Akin O, Franiel T, et al. Diffusion-weighted Endorectal MR Imaging at 3 T for Prostate Cancer: Tumor Detection and Assessment of Aggressiveness. Radiology 2011 Mar 24 [Epub ahead of print].

[23] Turkbey B, Pinto PA, Mani H, et al. Prostate cancer: Value of multiparametric MR imaging at 3 T for detection–histopathologic correlation. Radiology 2010;255:89–99.

[24] Puech P, Potiron E, Lemaitre L, et al. Dynamic contrast-enhanced-magnetic resonance imaging evaluation of intraprostatic prostate cancer: Correlation with radical prostatectomy specimens. Urology 2009; 74:1094–9.

[25] Kobus T, Hambrock T, Hulsbergen-van de Kaa CA, et al. In vivo assessment of prostate cancer aggressiveness using magnetic resonance spectroscopic imaging at 3 T with an endorectal coil. Eur Urol 2011 [Epub ahead of print].

[26] De Visschere PJ, De Meerleer GO, Futterer JJ, et al. Role of MRI in follow-up after focal therapy for prostate carcinoma. AJR 2010;194: 1427–33.

[27] Scheidler J, Hricak H, Vigneron DB, et al. Prostate cancer: Localization with three-dimensional proton MR spectroscopic imaging—clinicopathologic study. Radiol 1999;213:473–80.

[28] Kurhanewicz J, Vigneron DB, Hricak H, et al. Three-dimensional H-1 MR spectroscopic imaging of the in situ human prostate with high (0.24–0.7-cm3) spatial resolution. Radiology 1996;198:795–805.

[29] Riches SF, Payne GS, Morgan VA, et al. MRI in the detection of prostate cancer: Combined apparent diffusion coefficient, metabolite ratio, and vascular parameters. AJR 2009;193:1583–91.

[30] Klijn S, De Visschere PJ, De Meerleer GO, et al. Comparison of qualitative and quantitative approach to prostate MR spectroscopy in peripheral zone cancer detection. Eur J Radiol 2011 [Epub ahead of print].

[31] Scheenen TWJ, Futterer J, Weiland E, et al. Discriminating cancer from noncancer tissue in the prostate by three-dimensional proton magnetic resonance spectroscopic imaging. Invest Radiol 2011;46: 25–33.

[32] Riches SF, Payne GS, Morgan VA, et al. MRI in the detection of prostate cancer: Combined apparent diffusion coefficient, metabolite

ratio, and vascular parameters. AJR Am J Roentgenol 2009;193: 1583–91.
[33] Zakian KL, Sircar K, Hricak H, et al. Correlation of proton MR spectroscopic imaging with Gleason score based on step-section pathologic analysis after radical prostatectomy. Radiol 2005;234: 804–14.
[34] Rapp DE, Orvieto MA, Lucioni A, et al. Intra-operative prostate examination: Predictive value and effect on margin status. BJU Int 2005;96:1005–8.
[35] Labanaris AP, Zugor V, Takriti S, et al. The role of conventional and functional endorectal magnetic resonance imaging in the decision of whether to preserve or resect the neurovascular bundles during radical retropubic prostatectomy. Scand J Urol Nephrol 2009;43:25–31.
[36] Hricak H, Wang L, Wei DC, et al. The role of preoperative endorectal magnetic resonance imaging in the decision regarding whether to preserve or resect neurovascular bundles during radical retropubic prostatectomy. Cancer 2004;100:2655–63.
[37] Ogura K, Maekawa S, Okubo K, et al. Dynamic endorectal magnetic resonance imaging for local staging and detection of neurovascular bundle involvement of prostate cancer: Correlation with histopathologic results. Urology 2001;57:721–6.
[38] Lee SE, Hong SK, Han JH, et al. Significance of neurovascular bundle formation observed on preoperative magnetic resonance imaging regarding postoperative erectile function after nerve-sparing radical retropubic prostatectomy. Urology 2007;69:510–4.
[39] Margolis D, McClure T, Raman S, et al. Prostate MRI and surgical planning in robotic-assisted laparoscopic prostatectomy. Proceedings of the American Society of Clinical Oncology (ASCO) Genitourinary Cancers Symposium. San Francisco, CA: June 2010.
[40] Eastham JA, Kuroiwa K, Ohori M, et al. Prognostic significance of location of positive margins in radical prostatectomy specimens. Urology 2007;70:965–9.
[41] Epstein JI, Partin AW, Sauvageot J, et al. Prediction of progression following radical prostatectomy: A multivariate analysis of 721 men with long-term follow-up. Am J Surg Pathol 1996;20:286–92.
[42] Obek C, Sadek S, Lai S, et al. Positive surgical margins with radical retropubic prostatectomy: Anatomic site-specific pathologic analysis and impact on prognosis. Urology 1999;54:682–8.
[43] Smith JA Jr., Chan RC, Chang SS, et al. A comparison of the incidence and location of positive surgical margins in robotic assisted laparoscopic radical prostatectomy and open retropubic radical prostatectomy. J Urol 2007;178:2385–9, Discussion 2389–90.
[44] Patel VR, Shah S, Arend D. Histopathologic outcomes of robotic radical prostatectomy. Sci World J 2006;6:2566–72.
[45] Coelho RF, Chauhan S, Orvieto MA, et al. Influence of modified posterior reconstruction of the rhabdosphincter on early recovery of continence and anastomotic leakage rates after robot-assisted radical prostatectomy. Eur Urol 2011;59:72–80.
[46] Gautam G, Rocco B, Patel VR, et al. Posterior rhabdosphincter reconstruction during robot-assisted radical prostatectomy: Critical analysis of techniques and outcomes. Urology 2010;76:734–41.
[47] Villers A, Mcneal JE, Freihas FS, et al. Invasion of Denonvilliers' fascia in radical prostatectomy specimens. J Urol 1993;149:793–8.
[48] Al-Ahmadie HA, Tickoo SK, Olgac S, et al. Anterior-predominant prostatic tumors: Zone of origin and pathologic outcomes at radical prostatectomy. Am J Surg Pathol 2008;32:229–35.
[49] Lemaitre L, Puech P, Poncelet E, et al. Dynamic contrast-enhanced MRI of anterior prostate cancer: Morphometric assessment and correlation with radical prostatectomy findings. Eur Radiol 2009; 19:470–80.
[50] Amsellem-Ouazana D, Younes P, Conquy S, et al. Negative prostatic biopsies in patients with a high risk of prostate cancer. Is the combination of endorectal MRI and magnetic resonance spectroscopy imaging (MRSI) a useful tool? A preliminary study. Eur Urol 2005;47:582–6.
[51] Finley DS, Deane L, Rodriguez E, et al. Anatomic excision of anterior prostatic fat at radical prostatectomy: Implications for pathologic upstaging. Urology 2007;70:1000–3.
[52] Jeong J, Choi EY, Kang DI, et al. Pathologic implications of prostatic anterior fat pad. Urologic Oncol 2011 Mar 9 [Epub ahead of print].
[53] Borin JF, Skarecky DW, Narula N, et al. Impact of urethral stump length on continence and positive surgical margins in robot-assisted laparoscopic prostatectomy. Urology 2007;70:173–7.
[54] Ahlering TE, Eichel L, Edwards RA, et al. Robotic radical prostatectomy: A technique to reduce pT2 positive margins. Urology 2004; 64:1224–8.
[55] Park BJ, Sung DJ, Kim MJ, et al. The incidence and anatomy of accessory pudendal arteries as depicted on multidetector-row CT angiography: Clinical implications of preoperative evaluation for laparoscopic and robot-assisted radical prostatectomy. Korean J Radiol 2009;10:587–95.
[56] Nehra A, Kumar R, Ramakumar S, et al. Pharmacoangiographic evidence of the presence and anatomical dominance of accessory pudendal artery(s). J Urol 2008;179:2317–20.
[57] Box GN, Kaplan AG, Rodriguez E Jr., et al. Sacrifice of accessory pudendal arteries in normally potent men during robot-assisted radical prostatectomy does not impact potency. J Sex Med 2010; 7:298–303.
[58] Mulhall JP, Secin FP, Guillonneau B. Artery sparing radical prostatectomy—myth or reality? J Urol 2008;179:827–31.
[59] Nguyen L, Jhaveri J, Tewari A. Surgical technique to overcome anatomical shortcoming: Balancing post-prostatectomy continence outcomes of urethral sphincter lengths on preoperative magnetic resonance imaging. J Urol 2008;179:1907–11.
[60] Mason BM, Hakimi AA, Faleck D. The role of preoperative endorectal coil magnetic resonance imaging in predicting surgical difficulty for robotic prostatectomy. Urology 2010;76:1130–5.
[61] von Bodman C, Matsushita K, Matikainen MP, et al. Do pelvic dimensions and prostate location contribute to the risk of experiencing complications after radical prostatectomy? BJU Int 2011 Mar 28 [Epub ahead of print].
[62] Mendoza PJ, Stern KJM, Jaffe W, et al. Pelvic anatomy on preoperative magnetic resonance imaging can predict early continence after robot-assisted radical prostatectomy. J Endourol 2011;25:51–5.
[63] Saokar A, Islam T, Jantsch M, et al. Detection of lymph nodes in pelvic malignancies with computed tomography and magnetic resonance imaging. Clin Imaging 2010;34:361–6.
[64] Finley DS, Rodriguez E Jr., Ahlering TE. Combined inguinal hernia repair with prosthetic mesh during transperitoneal robot assisted laparoscopic radical prostatectomy: A 4-year experience. J Urol 2007; 178:1296–9, Discussion 1299–300.
[65] Marien T, Taouli B, Telegrafi S, et al. Optimizing the detection of subclinical inguinal hernias in men undergoing open radical retropubic prostatectomy. BJU Int 2010;106:1468–72.
[66] Angulo JC, Romero I, Cabrera P, et al. Vesiculectomy with laparoscopic partial prostatectomy in the treatment of primary adenocarcinoma of the seminal vesicle with carcinomatous transformation of the ejaculatory duct. Actas Urol Esp 2011;35:304–9.
[67] Marien TP, Shapiro E, Melamed J, et al. Management of localized prostate cancer and an incidental ureteral duplication with upper pole ectopic ureter inserting into the prostatic urethra. Rev Urol 2008;10: 297–303.